Latin American Journal of Aquatic Research, 52(2): 270-288, 2024
DOI: 10.3856/vol52-issue2-fulltext-3103

Research Article

Performance of high-resolution MUR satellite sea surface temperature data as a proxy for near-surface *in situ* temperatures on neotropical reefs

Fiona Skerrett[1], Anne Adelson[2] & Rachel Collin[1]
[1]Smithsonian Tropical Research Institute, Balboa Ancon, Panama
[2]Scripps Institution of Oceanography, University of California San Diego
La Jolla, California, USA
Corresponding author: Fiona Skerrett (fskerrett@wesleyan.edu)

ABSTRACT. As ocean temperatures increase, so does the need for accurate, regular, and widespread temperature data. This is especially important for researchers studying corals, which can be pushed over their bleaching thresholds by small, sustained changes in water temperature. Satellite data products offer longitudinal estimates of sea surface temperature (SST) taken at regular intervals without the ongoing costs and geospatial limits associated with underwater temperature loggers. However, previous work indicates satellite data are sometimes characterized by significant temperature biases, particularly in stratified coastal waters. Here, we compared the foundation sea surface temperature (fSST) estimated from a highly processed, gridded satellite data set (GHRSST MUR L4 Global SST) to *in situ* temperature (IST) data collected from coral reef habitats in the top 20 m of the water column at 19 sites in Panama. Comparisons between Pacific and Caribbean coasts and between upwelling and non-upwelling seasons provide a robust test of the utility of this product to estimate subsurface temperatures. The mean differences between fSST and IST show that MUR fSST accurately reflects temperatures at shallow (<9 m) depths on the Caribbean coast (mean bias ≤0.55°C ± standard error (SE) 0.01°C) and during the non-upwelling season on the Pacific coast (mean bias ≤0.26°C ± SE 0.03°C). MUR fSST poorly reflects IST during the Pacific upwelling season, especially at sites 12 m and deeper. In such cases, 66% of satellite estimates deviated from ISTs by >1°C. Our findings underscore how highly processed SST data products should be ground-truthed before being used as a substitute for IST, especially in upwelling areas.

Keywords: sea surface temperature; thermal tolerance; remote sensing; upwelling; Panama

INTRODUCTION

Rising global sea surface temperatures extensively affect coral reef diversity and the biological processes within reef communities (Hughes et al. 2018, Bahr et al. 2020, Cyronak et al. 2020, Cornwall et al. 2021). Corals often live close to their thermal maxima, and slight temperature increases can trigger bleaching and coral death (Lough et al. 2018). In addition to relying on healthy coral reefs for habitat, many tropical coastal organisms are also sensitive to increased ocean temperatures (Vinagre et al. 2018). Researchers and coastal ecosystem managers must have reliable and accurate temperature measurements from the depths inhabited by these communities to understand the distribution of marine animals relative to the actual thermal conditions they experience (Castillo & Lima 2010, Bailey et al. 2019, Benway et al. 2019, Hemming et al. 2020).

Biologists and oceanographers commonly use *in situ* temperature (IST) loggers to monitor temperatures at their study sites. Although this facilitates accurate measurement of temperatures at a particular site that

Associate Editor: Andrea Piñones

can be linked directly to organismal performance, this approach has limitations. Obtaining temperatures from several sites and depths can require significant investment in loggers and incur the costs associated with instrument deployment, recovery, and servicing (Contractor & Roughan 2021). Adequately characterizing ISTs can be particularly challenging in dynamic coastal environments, upwelling sites, and biogeographic boundaries, where complex oceanographic processes can result in spatial and temporal heterogeneity in temperature (Leichter et al. 2006, 2012, Smale & Wernberg 2009, Woo & Park 2020). *In situ* loggers may be particularly advantageous at detecting temperature variation that results from diurnal cycles, internal waves, and other processes that occur on fine temporal scales (Leichter et al. 2006, 2012, DeCarlo et al. 2015, Colin & Johnston 2020, Lee et al. 2020, Wyatt et al. 2020). However, the most accessible and affordable loggers may produce temperature estimates that are too imprecise for some applications.

Satellite data products are frequently used as an alternative to *in situ* monitoring because they offer real-time monitoring of coastal temperatures over large areas (Liu et al. 2014, Hedley et al. 2016). These datasets are generated from infrared readings of the surface skin of the ocean taken by orbiting satellites, resulting in a temporal resolution that is typically coarser than can be achieved with *in situ* loggers. Satellite sea surface temperature (SST) datasets undergo differing degrees of data processing, which range from calibrated raw data (Level 1) to gridded and interpolated models based on blended data products that may contain both infrared and microwave data (Level 4) (Dash et al. 2012, Chin et al. 2017). As ecologists adopt these higher-level products, it is vital to understand how well they reflect temperatures experienced by the ecological communities of interest. This is particularly important in coastal zones, where complex oceanographic processes and heterogeneous environmental conditions influence benthic and pelagic ecosystems (Toth et al. 2017). Satellite data can have either a warm or cold bias compared to temperatures from *in situ* loggers in coastal areas, depending on the dynamics of the site (Castillo & Lima 2010, Dufois et al. 2012, Peres et al. 2017, Claar et al. 2019, Gomez et al. 2020, Pereira et al. 2020, Woo & Park 2020). These biases may be due to vertical mixing near coastal boundaries (Stobart et al. 2015, Woo & Park 2020). Because the performance of SST estimates depends on the peculiarities of a particular site and may be impacted by cloud masking, thermal emissions from the land, air temperature inversions, and fine-scale oceanographic processes (Peres et al. 2017, Gomez et al. 2020, Pereira et al. 2020), it is important to understand their performance for a specific location before they are applied instead of *in situ* data.

The Isthmus of Panama is one complex region of particular interest to coral reef biologists, where extensive IST datasets are unavailable. The monsoonal climate in Panama is driven by seasonal oscillations of the Intertropical Convergence Zone (ITCZ) (O'Dea et al. 2012). When the ITCZ is to the south, Panama experiences low rainfall and strong northerly winds (O'Dea et al. 2012, Sellers et al. 2021). These winds give rise to upwelling along the Pacific coast, while uneven terrestrial topography and complex island groups drive spatial variability in the intensity of upwelling (D'Croz & O'Dea 2007, Gomez et al. 2017, Toth et al. 2017). The Cordillera Central mountain range in western Panama somewhat blocks the wind, reducing wind in the Gulf of Chiriquí compared to the more eastern Gulf of Panama (D'Croz & O'Dea 2007, O'Dea et al. 2012, Randall et al. 2020). During the rest of the year, the ITCZ lies over Panama, subjecting the country to heavy rains, weaker winds, and a cessation of upwelling. Shallow subsurface temperatures in the Pacific average 28.6°C in the non-upwelling season and can fall significantly below 20°C during vigorous upwelling (Robertson & Collin 2015, Enochs et al. 2021). Possibly because it is protected from cold, acidic, and hypoxic waters, the development of coral reefs in the Gulf of Chiriquí is more extensive (D'Croz & O'Dea 2007, Manzello et al. 2008, Gomez et al. 2017, Toth et al. 2017).

In contrast, temperatures in the shallow surface waters of the Caribbean coast are relatively stable, with seasonal fluctuations between 27-31°C (Kaufmann & Thompson 2005, Robertson & Collin 2015, Collin & Chan 2016, Lucey et al. 2021, Adelson et al. 2022). These temperatures sustain well-developed coral communities that have been documented in detail from Bocas del Toro (Guzmán 2003, Dominici-Arosemena & Wolff 2005, Seemann et al. 2013, Rodas et al. 2020) in the northwest, along the northeast coast near the city of Colón (Guzmán et al. 2020), and along the San Blas Archipelago (Shulman & Robertson 1996, Guzmán 2003, Andréfouët & Guzmán 2005). In years when the Caribbean is particularly warm, coral bleaching occurs on these reefs (Gardner et al. 2003, Neal et al. 2017).

IST data are limited near the Panamanian coast, with available data distributed patchily across depths and geographic locations. We used published *in situ* datasets with durations of >1 year from both coasts of Panama (Fig. 1) to assess the performance of a Level 4

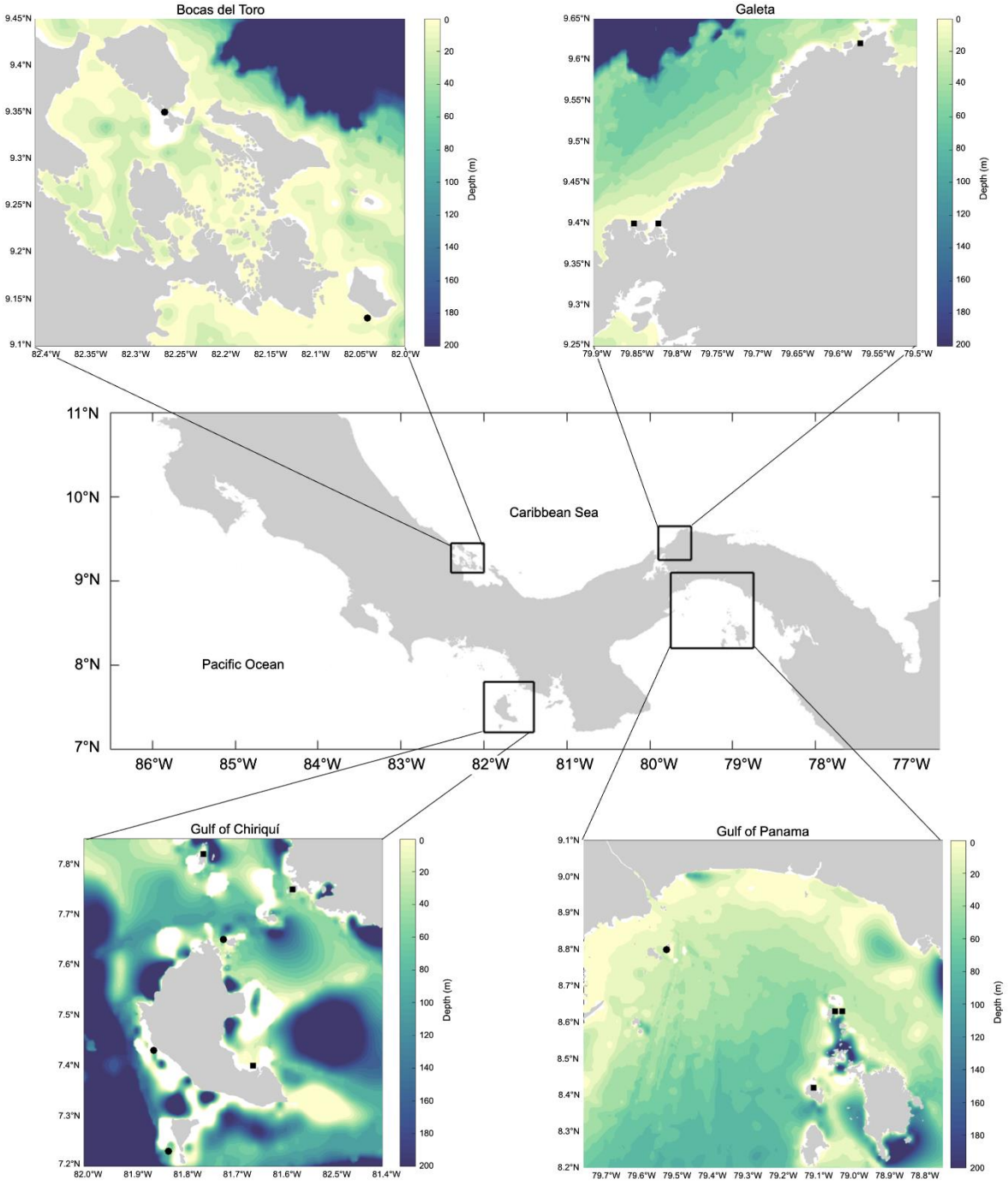

Figure 1. Map of four chosen regions (Bocas del Toro, Galeta, Gulf of Chiriquí, Gulf of Panama) and sites. The circle site marker indicates a depth of 3 m, and the square marker indicates a depth of >3 m. The color gradient indicates water depth.

data product, the GHRSST Level 4 MUR Global Foundation Sea Surface Temperature Analysis (v4.1). This data set is unique in that instead of directly measuring ocean skin temperature; it estimates foundation SST (fSST), the ocean temperature unaffected by the diurnal warming cycle. fSST is modeled as occurring early in the day, before diurnal warming, or at a depth at which sunlight does not penetrate (https://www.ghrsst.org/ghrsst-data-services/products/). MUR uses nighttime SST data from a variety of Level 2 and 3 satellite data products and measurements from the NOAA *In Situ* Quality

Monitoring project (iQuam) to model foundation ocean temperatures on a spatially and temporally dense, gap-free global grid (Dash et al. 2012, JPL MUR MEASUREs Project 2015, Chin et al. 2017). Therefore, this data product may be more effective at capturing water temperatures at depths relevant to many coral reefs than data products that estimate skin temperature. MUR has been previously compared with shallow (≤0.5 m depth) IST in three sub-tropical regions (Vazquez-Cuervo et al. 2019, Pereira et al. 2020, Woo & Park 2020). Each study observed a positive temperature bias for MUR estimates, with Pereira et al. (2020) documenting a notably stronger bias during upwelling days in upwelling zones in southeastern Brazil. To our knowledge, MUR fSST has not been applied in the tropics at depths greater than 0.5 m. Identifying the conditions under which MUR provides a high-quality estimate of coastal ISTs will allow coral reef biologists and coastal ecologists to utilize this tool most effectively and appropriately.

Here, we specifically examine how well MUR data perform across sites and depths inhabited by coral reef communities in Panama. We seek to answer a) whether MUR fSST is a better approximation of the temperature measured by loggers at deeper sites than near the surface and b) how well MUR estimates ISTs under the challenging oceanographic conditions associated with seasonal upwelling in Panama.

MATERIALS AND METHODS

Study sites

Nineteen locations on or near coral reefs surrounding Panama where IST data have previously been collected were used to study the agreement between satellite estimates of fSST and ISTs (Fig. 1). The sites span both the Caribbean and Pacific coasts and represent varying distances from the mainland and a range of seasonal upwelling intensities. They were grouped into four regions (Table 1). On the Caribbean coast, the regions were the Bahía Almirante in Bocas del Toro Province and between the city of Colón and the Costa Arriba in Colón Province, subsequently referred to as Bocas del Toro and Galeta, respectively (Fig. 1). On the Pacific coast, the regions were the area in the Gulf of Chiriquí around Coiba Island and the Gulf of Panama between Panama City and the Perlas Islands, referred to, respectively, as the Gulf of Chiriquí and the Gulf of Panama (Fig. 1).

Satellite data

High-resolution satellite estimates of fSST from the GHRSST Level 4 MUR Global Foundation SST Analysis v4.2 dataset (https://coastwatch.pfeg.noaa.gov/erddap/griddap/jplMURSST41.html) were compared with IST data at all 19 sites. This dataset incorporates nighttime inputs from four satellite products. It calibrates these with IST data to estimate daily fSSTs at an extremely high spatial resolution (0.01° latitude×0.01° longitude / 1.1×1.1 km resolution) (JPL MUR MEASUREs Project 2015, Chin et al. 2017, Woo & Park 2020). These inputs are sourced from the Moderate-Resolution Imaging Spectroradiometer (MODIS) and ASMR-E sensors aboard Aqua, MODIS on Terra, WindSat on Coriolis, and Advanced Very High-Resolution Radiometer (AVHRR) aboard the platform NOAA-19. When combined according to the MUR methodology, these data inputs inform estimates of foundation ocean temperatures (Dash et al. 2012, JPL MUR MEASUREs Project 2015, Chin et al. 2017). Daily MUR fSST was downloaded for each site to compare with logger data.

In situ data

Data published by the Smithsonian Tropical Research Institute's (STRI) environmental monitoring program (https://biogeodb.stri.si.edu/physical_monitoring/research/sst) and Florida Institute of Technology/United States Geological Survey (https://www.bco-dmo.org/dataset/776478) were used as our IST dataset. These data were obtained using Onset HOBO Pro v2 temperature loggers (±0.2°C) for every site except BDT, consistent across both data sources (Randall et al. 2020; https://biogeodb.stri.si.edu/physical_monitoring/research/sst). Temperatures collected at BDT (1 m) were obtained using a Campbell Scientific Model 107 temperature probe (±0.2°C) attached to a permanent platform (https://biogeodb.stri.si.edu/physical_monitoring/downloads/Temperature_Probe_Model_107.pdf). All Hobo loggers were deployed on the benthos and attached to hard substrates between 2 and 18.3 m deep. In the case of the Bocas del Toro region, five loggers collected data at different depths at the same geographic coordinates. The datasets differed in duration, but we used all available temperature data between 2009 and 2020 to increase the likelihood that both El Niño and La Niña conditions were captured.

Each logger was sampled at 15- or 30-min intervals, although the timestamps were often offset from the hour. Since MUR estimates fSST without diurnal warming, MUR data are timestamped early in the day. The timestamp corresponds to 04:00 h in Panama, which observes the UTC-5 time zone. Daily IST was extracted from each site at the closest timestamp to

Table 1. Summary of the sites where *in situ* water temperatures were recorded, showing the region of Panama, depth, temporal range, and source of the data.

Location	Coordinates	Depth (-m)	Date Range	Source
		Caribbean Sea		
Galeta				
Galeta Channel (GAL)	9.40°N, 79.85°W	3	01/09 - 12/20	Smithsonian Tropical Research Institute
Isla Grande (GRA)	9.62°N, 79.57°W	3	01/09 - 06/19	Smithsonian Tropical Research Institute
Bahía Las Minas (BAH)	9.40°N, 79.82°W	3	01/09 - 12/20	Smithsonian Tropical Research Institute
Bocas del Toro				
Bocas del Toro Platform (BDT)	9.35°N, 82.26°W	1	01/09 - 12/20	Smithsonian Tropical Research Institute
Isla Colón Seagrass (SEA)	9.35°N, 82.26°W	2	01/09 - 12/20	Smithsonian Tropical Research Institute
Isla Colón (IC5)	9.35°N, 82.26°W	4.6	01/09 - 12/20	Smithsonian Tropical Research Institute
Isla Colón (IC9)	9.35°N, 82.26 W	9.1	01/09 - 12/20	Smithsonian Tropical Research Institute
Isla Colón (IC18)	9.35°N, 82.26°W	18.3	01/09 - 12/20	Smithsonian Tropical Research Institute
Cayo Agua (ICA)	9.13°N, 82.04°W	5.2	01/09 - 12/20	Smithsonian Tropical Research Institute
		Pacific Ocean		
Gulf of Chiriquí				
Coiba (COI)	7.40°N, 81.66°W	3	03/16 - 03/18	Florida Institute of Technology, US Geological Survey, Woods Hole Oceanographic Institution
Canales de Tierra (CAN)	7.75°N, 81.58°W	3	03/16 - 03/18	Florida Institute of Technology, US Geological Survey, Woods Hole Oceanographic Institution
Uva (UVA)	7.82°N, 81.76°W	3	03/16 - 03/18	Florida Institute of Technology, US Geological Survey, Woods Hole Oceanographic Institution
Isla Coiba Frijoles (FRI)	7.65°N, 81.72°W	18.3	06/09 - 11/11	Smithsonian Tropical Research Institute
Isla Coiba Roca Hacha (ROC)	7.43°N, 81.86°W	18.3	06/09 - 01/16	Smithsonian Tropical Research Institute
Isla Jicarón Catedral (CAT)	7.23°N, 81.83°W	18.3	06/09 - 02/16	Smithsonian Tropical Research Institute
Gulf of Panama				
Isla Taboguilla (TAB)	8.80°N, 79.52°W	12	01/09 - 12/20	Smithsonian Tropical Research Institute
Contadora (CON)	8.63°N, 79.03°W	3	03/16 - 03/18	Florida Institute of Technology, US Geological Survey, Woods Hole Oceanographic Institution
Saboga (SAB)	8.63°N, 79.05°W	3	03/16 - 03/18	Florida Institute of Technology, US Geological Survey, Woods Hole Oceanographic Institution
Pedro González (PED)	8.42°N, 79.11°W	3	03/16 - 03/18	Florida Institute of Technology, US Geological Survey, Woods Hole Oceanographic Institution

04:00 h within a 13-min buffer to draw comparisons with the MUR data. Therefore, the single temperature recorded between 03:47 and 04:13 h each day was treated as the daily *in situ* value for 04:00 h.

Analysis

We used two metrics to determine how the fSST differed from the IST: the mean (and standard error) of the daily temperature differences (DTDs) between fSST and IST and the regression slope between IST and fSST. Each metric was also calculated independently for the non-upwelling and upwelling seasons to determine if seasonal differences in coastal oceanography alter the utility of the fSST to characterize IST. Based on historical climate patterns (Sellers et al. 2021), we defined the dry, upwelling season as January 1-April 30, and the wet, non-upwelling season as June 1-November 30. December and May were treated as transition months and removed from our seasonal analyses to avoid errors due to inaccurate attribution to upwelling or non-upwelling seasons. DTDs were calculated, and linear regressions were run for each location during the upwelling and non-upwelling seasons.

DTDs were calculated for each site as [fSST-IST]. Positive values indicated that satellite estimates were

warmer than *in situ* measures, while negative values showed that satellite estimates were underestimating the ISTs. Mean DTDs reflect systematic bias in the temperatures, while the standard error reflects the variation around this estimate. The DTD was not calculated for the days when fSST or IST was unavailable. Summary statistics, including skew, kurtosis, minimum, median, and maximum, were calculated for DTDs at each site across the total dataset and by season and are provided in the Supplementary data (Table S1). To understand how seasonality and location affected satellite and IST differences, DTDs were averaged per site throughout the period and month (Table 2, S2).

The slope of the regression line of fSST on IST indicates if the differences between the estimates are temperature-dependent. A slope of 1 shows that any difference is the same across the observed temperature range. In contrast, a slope of <1 shows that the fSST values are biased downwards at higher temperatures compared to lower temperatures. Conversely, a slope of >1 shows that values are biased upwards at higher temperatures compared to lower temperatures. Low R^2 values reflect more noise or error of the estimate in the relationship between fSST and IST.

RESULTS

Spatial patterns in mean DTD of MUR

Overall, the MUR fSST and IST showed small differences (<0.55ºC) for sites in the Caribbean and at shallow sites in the Pacific (Table 2, Figs. 2, 4). The overall average DTD for our Caribbean sites was negative (mean DTD_{Avg} = -0.30ºC; SE = 0.05ºC), showing a pattern of lower fSST temperature estimates compared to IST measurements. DTD was similarly small but positive for shallow sites in the Pacific (mean DTD_{Avg} = 0.17ºC; SE = 0.08ºC) (Table 2), showing a pattern of higher fSST estimates compared to ISTs. These subtle biases are of a magnitude similar to the instrument error of the loggers, which was ±0.2ºC for the *in situ* measurements (Randall et al. 2020; https://biogeodb.stri.si.edu/physical_monitoring/research/sst). While there is no comparable instrument error for MUR fSST, estimates of standard deviation provided with the temperature data range from 0.37 to 0.42ºC (https://coastwatch.pfeg.noaa.gov/erddap/griddap/jplMURSST41.html), implying that 95% of MUR fSST estimates fall within 0.74 or 0.84ºC of the true value. Nevertheless, the consistent difference in the direction of the DTD across sites in each ocean suggests that MUR data may subtly underestimate *in situ* ocean temperatures compared to fSST on reefs in the Caribbean and subtly overestimate ISTs compared to fSST in the shallow Pacific.

Unlike in the Caribbean and shallow Pacific waters, we observed a considerable temperature difference between the fSST and IST in the Pacific sites at 12 m and deeper (Isla Taboguilla: TAB, Isla Coiba Frijoles: FRI, Isla Coiba Roca Hacha: ROC, Isla Jicarón Catedral: CAT; Figs. 2, 4). The mean DTD for these four sites was 1.23 ± SE 0.08ºC, suggesting that MUR data considerably overestimate *in situ* water temperatures at deep sites. To determine if this mismatch is due to seasonal upwelling, we conducted paired *t*-tests on mean DTD at each site, paired across the two seasons. At the deep Pacific sites, mean DTD differed significantly between the two seasons (paired *t*-test: t = 6.25; n = 4; $P < 0.01$), and, in all cases, the mean temperature bias was higher in the upwelling season (Table 2). In addition, the DTD distributions are skewed right in the upwelling season (Fig. 4) to the extent that on some days, the DTD could be 10ºC or higher (Table 2). We found no such significant seasonal effect on mean difference in the shallow Pacific sites (paired *t*-test: t = 2.51; n = 6; P = 0.05) or in the Caribbean (paired *t*-test: t = 1.88; n = 9; P = 0.10), where there is no upwelling and where DTD is less skewed (Fig. 3, Table S1).

Temperature dependence of bias

Linear regressions revealed that the regression slope of fSST on IST for all of our sites is less than 1 (Table 3). Scatter plots in Figures 5-6 show that the regressions generally cross the 1:1 reference line within the range of the observed temperatures, revealing that, in general, the SST bias is temperature-dependent and that satellite estimates are cool-biased at higher logged temperatures and warm-biased at lower logged temperatures relative to IST. However, this pattern differs somewhat by region.

Scatter plots illustrate that at the Gulf of Chiriquí, Gulf of Panama, and Galeta Channel (GAL) in Galeta, fSSTs overestimated at lower ISTs (Figs. 5a, 6a-b). At all Galeta sites, fSSTs also underestimated at higher ISTs (Fig. 5a). At Bocas del Toro, the temperature dependence of bias was minimal. These sites showed slopes that were nearly identical to the 1:1 reference line, with departures generally within the 0.2ºC of instrument error (Table 3, Fig. 5b). Linear models of fSST on IST in the Gulf of Panama were also typically strong overall, with $R^2 \geq 0.85$ (Table 3).

A strong seasonal signal in the Galeta region caused a vertical offset between regression lines for the two

Table 2. Summary of the daily temperature differences (DTDs) between logger and MUR satellite data for 19 loggers from Panama's Pacific and Caribbean coasts. Bolding indicates a mean DTD for which the DTD is greater than the ±0.2°C instrument error of the loggers. SE: standard error.

Location	Depth (-m)	DTD				
		Overall			Upwelling	Non-upwelling
		Mean ± SE (°C)	Min (Logger > Sat)	Max (Sat > Logger)	Mean ± SE (°C)	Mean ± SE (°C)
Caribbean Sea						
Galeta						
Galeta Channel	3	-0.08 ± 0.01	-2.39	2.35	-0.13 ± 0.01	-0.06 ± 0.01
Isla Grande	3	**-0.32** ± 0.01	-2.04	1.98	**-0.39** ± 0.01	**-0.27** ± 0.01
Bahía Las Minas	3	**-0.55** ± 0.01	-2.27	1.67	**-0.68** ± 0.01	**-0.49** ± 0.01
Bocas del Toro						
Bocas del Toro Platform	1	**-0.24** ± 0.01	-2.13	2.75	-0.16 ± 0.01	**-0.31** ± 0.01
Isla Colón Seagrass	2	-0.19 ± 0.01	-2.08	2.85	-0.08 ± 0.01	**-0.26** ± 0.01
Isla Colón	4.6	**-0.21** ± 0.01	-2.71	2.12	-0.12 ± 0.01	**-0.30** ± 0.01
Isla Colón	9.1	**-0.31** ± 0.01	-2.70	2.08	-0.12 ± 0.01	**-0.47** ± 0.01
Isla Colón	18.3	**-0.39** ± 0.01	-3.31	2.20	-0.06 ± 0.01	**-0.62** ± 0.01
Cayo Agua	5.2	**-0.44** ± 0.01	-3.35	1.89	**-0.25 ± 0.01**	**-0.59** ± 0.01
Pacific Ocean						
Gulf of Chiriquí						
Coiba	3	-0.13 ± 0.02	-1.85	2.43	-0.04 ± 0.04	-0.26 ± 0.03
Canales de Tierra	3	0.00 ± 0.03	-1.53	3.70	-0.04 ± 0.06	-0.09 ± 0.03
Uva	3	**0.23** ± 0.02	-1.41	4.01	0.18 ± 0.04	0.20 ± 0.03
Isla Coiba Frijoles	18.3	**1.03** ± 0.05	-1.47	9.35	**1.79** ± 0.13	**0.69** ± 0.04
Isla Coiba Roca Hacha	18.3	**1.41** ± 0.04	-1.48	10.77	**3.06** ± 0.10	**0.72** ± 0.03
Isla Jicarón Catedral	18.3	**1.25** ± 0.03	-1.29	11.01	**2.68** ± 0.08	**0.54** ± 0.02
Gulf of Panama						
Isla Taboguilla	12	**1.23** ± 0.026	-2.66	10.03	**2.94** ± 0.05	**0.36** ± 0.01
Contadora	3	0.19 ± 0.03	-1.66	5.06	**0.51** ± 0.07	0.01 ± 0.03
Saboga	3	**0.42** ± 0.04	-1.35	6.42	**1.06** ± 0.08	0.08 ± 0.03
Pedro González	3	**0.33** ± 0.03	-1.72	5.18	**0.92** ± 0.08	0.01 ± 0.03

seasons. In Galeta, fSST estimates of the same IST were up to 1°C higher in the non-upwelling season than in the upwelling season (Fig. 5a). There was also a seasonal bias offset at the deep Gulf of Chiriquí sites, where MUR estimates were higher in the upwelling season than in the non-upwelling season for the same IST (Fig. 6a). Linear regressions for Gulf of Chiriquí and Gulf of Panama sites showed slopes consistently closer to 1 in the non-upwelling season. Canales de Tierra (CAN) is an exception to this trend (m_{Up} = 0.47, $m_{Non\text{-}Up}$ = 0.41), though the CAN sample size was smaller than that of other sites (n = 410; Table 3, Fig. 2). Seasonality had little effect on the temperature dependence of bias for the Bocas del Toro sites. The non-upwelling and upwelling season regression lines for these sites had similar slopes across seasons (Table 3, Fig. 5b). Two exceptions to the above trend were Isla Colón (IC18) and Cayo Agua (ICA), which indicated seasonal signals with a flatter slope in the non-upwelling season (m_{Up} = 0.81, $m_{Non\text{-}Up}$ = 0.58 and m_{Up} = 0.91, $m_{Non\text{-}Up}$ = 0.67, respectively).

Under what circumstances can fSST accurately estimate IST?

The acceptable accuracy of IST estimates will vary depending on the nature of the research. However, our data indicated that MUR more consistently estimated accurate Caribbean temperatures than Pacific temperatures. MUR estimates were within 1.0°C of ISTs 89% of days in the Caribbean, compared to 69% in the Pacific. In fact, at the deep Gulf of Chiriquí sites and Isla Taboguilla (TAB), 21% of the days had a DTD > 2.0°C, and 5% had a DTD > 5.0°C. Further, the average DTD range of the deep Gulf of Chiriquí sites (FRI, ROC, CAT) was over twice that of IC18 in the Caribbean despite the equivalent depth of the sites (Table 2, Figs. 3b-4a).

DISCUSSION

The number and sophistication of available satellite data products estimating ocean temperature is growing (Hedley et al. 2016), but only a few Level 2 or 3 pro-

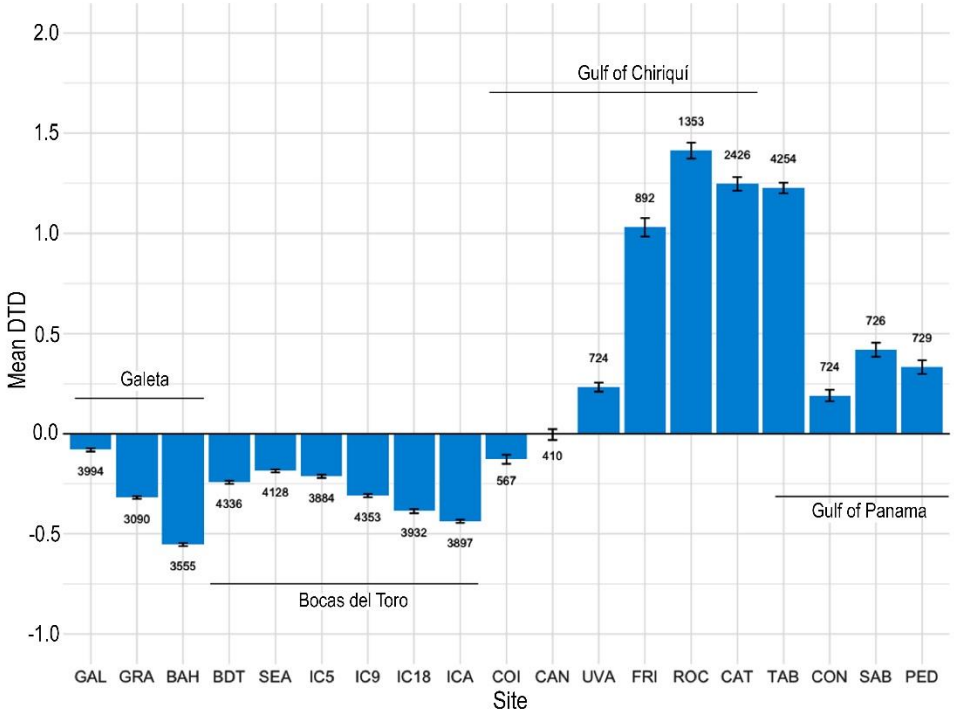

Figure 2. Mean daily temperature difference (DTD) of MUR ± standard error in sites grouped by region. A value above or below each bar is the number of temperature data points (N). GAL: Galeta, GRA: Isla Grande, BAH: Bahía Las Minas, BDT: Bocas del Toro Platform, SEA: Isla Colón Seagrass, IC5: Isla Colón 4.6 m, IC9: Isla Colón 9.1 m, IC18: Isla Colón 18.3 m, ICA: Cayo Agua, COI: Coiba, CAN: Canales de Tierra, UVA: Uva, FRI: Isla Coiba Frijoles, ROC: Isla Coiba Roca Hacha, CAT: Isla Jicarón Catedral, TAB: Isla Taboguilla, CON: Contadora, SAB: Saboga, PED: Pedro González.

ducts have been evaluated across a variety of locations and oceanographic conditions for their capacity to estimate coastal temperatures accurately (Pearce et al. 2007, Castillo & Lima 2010, Smit et al. 2013, Claar et al. 2019). Our results confirm that a Level 4 satellite data product, GHRSST MUR L4 Global SST, performs adequately as an alternative to *in situ* data monitoring for some uses for shallow waters in Panama. Overall, the MUR estimates were within 1°C of logged temperatures 83% of the time and were within 0.5ºC 60% at the 3 m sites in the Pacific and the Caribbean. However, the accuracy with which MUR temperatures reflect reef temperatures depends on the oceanographic characteristics of the nearshore environment. MUR estimates differed substantially from logged temperatures at the 12-18 m sites, especially during the upwelling season. This demonstrates that MUR is a fairly good proxy for ISTs during all but the upwelling periods.

Large discrepancies between satellite-derived SSTs and ISTs during upwelling have been previously reported for other regions and other data products. Results from analyses of Pathfinder SST data in the four major Eastern Boundary Upwelling Systems found large differences. However, this could be attributed to filtering unusually cold readings from the dataset (Dufois et al. 2012). Likewise, three different Level 4 data products failed to reflect drops in surface temperatures measured by buoys during upwelling off the coast of southern Brazil (Pereira et al. 2020). This difficulty in modeling water temperature below the surface skin during upwelling is unfortunate, as a satellite data product that accurately models ocean temperature in upwelling areas would be invaluable to biologists. Upwelling areas are some of the most productive coastal areas, as upwelling drives phytoplankton blooms, which are critically important for coastal ecosystems and fisheries (Largier 2020). However, upwelling events are also associated with hypoxic events and reductions in pH (Grantham et al. 2004). Reduced temperatures due to upwelling also shape the abundance and distribution of coral communities in the tropical eastern Pacific, as temperatures can drop below viable ranges for corals (<18°C; Furnas 2011), which can thin the frameworks of coral reefs and decrease the maximum depth at which corals develop (D'Croz & O'Dea 2007, Toth et al. 2017). For these reasons, it would be valuable to

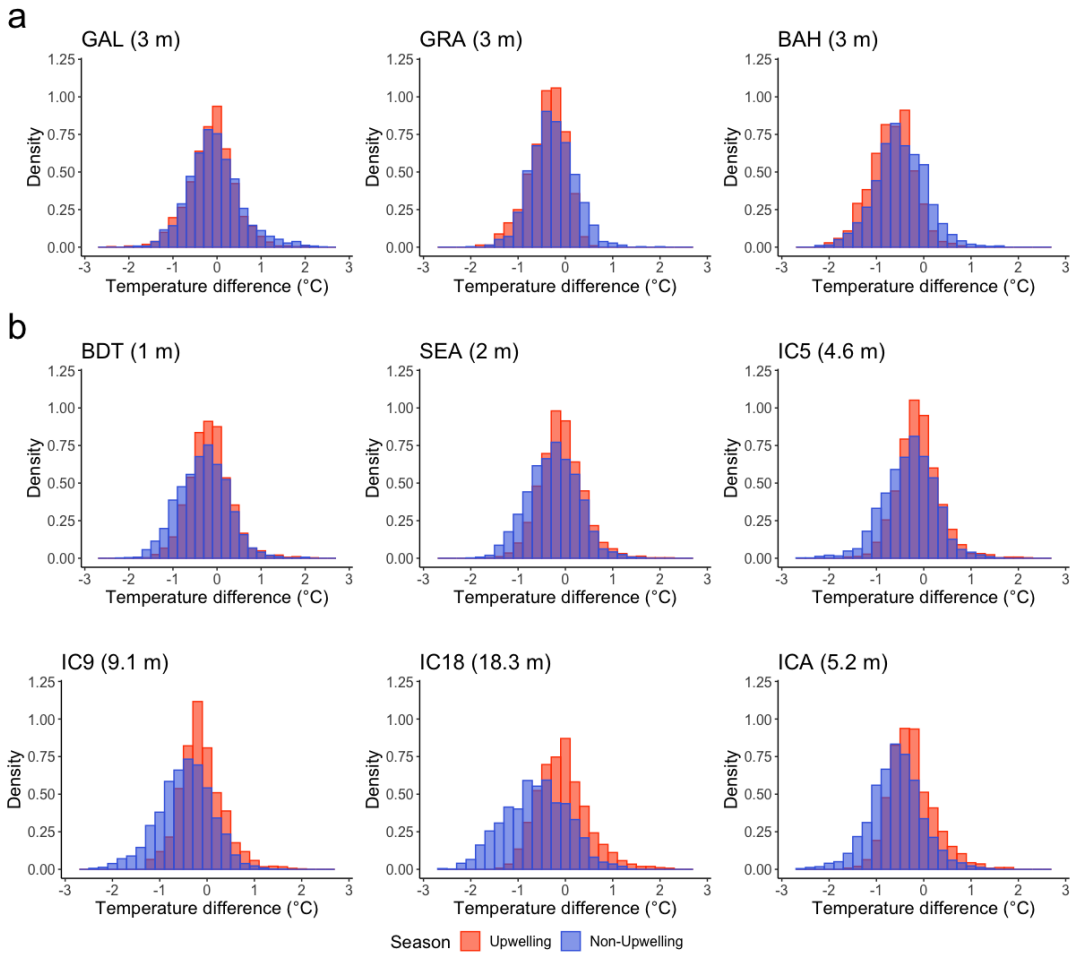

Figure 3. Density plot of daily temperature differences ([fSST - IST]), separated by season for sites in the Caribbean. a) Galeta and b) Bocas del Toro. GAL: Galeta, GRA: Isla Grande, BAH: Bahía Las Minas, BDT: Bocas del Toro Platform, SEA: Isla Colón Seagrass, IC5: Isla Colón 4.6 m, IC9: Isla Colón 9.1 m, IC18: Isla Colón 18.3 m, ICA: Cayo Agua, COI: Coiba, CAN: Canales de Tierra, UVA: Uva, FRI: Isla Coiba Frijoles, ROC: Isla Coiba Roca Hacha, CAT: Isla Jicarón Catedral, TAB: Isla Taboguilla, CON: Contadora, SAB: Saboga, PED: Pedro González.

assess how well MUR data in other upwelling regions capture upwelling, as greater coverage from buoys and more well-developed oceanographic models for well-studied regions may result in better agreement between MUR fSST and *in situ* data.

The accuracy of MUR estimates of IST also depends on the temperature. Most importantly, MUR underestimate IST at the higher end of the temperature range at our sites. At ISTs higher than ~29°C, MUR estimates were consistently lower than ISTs. These temperatures are close to the thermal limits of many tropical shallow-water organisms, including sea urchins, seagrasses, fishes, and corals, which have thermal safety limits of only a few degrees at these high temperatures (Savva et al. 2018, Collin et al. 2021, Bennett et al. 2022, Klepac & Barshis 2022, Marbà et al. 2022). When exposed to multiple stressors, like deoxygenation, thermal safety margins can be reduced further (Lucey et al. 2021, Alderdice et al. 2022). Accurate assessments of environmental temperatures near these thresholds are vital for understanding real-world thermal tolerances under field conditions. Since MUR temperatures are calculated using nighttime SST and underestimated IST when temperatures are high, reliance on only satellite-derived fSST risks crucially underestimating the thermal stress experienced by organisms in shallow tropical waters.

Our findings have important implications for researchers planning to use MUR data to track temperatures in coral reef ecosystems. The results corroborate existing findings that satellite datasets are not always adequate substitutions for IST monitoring in

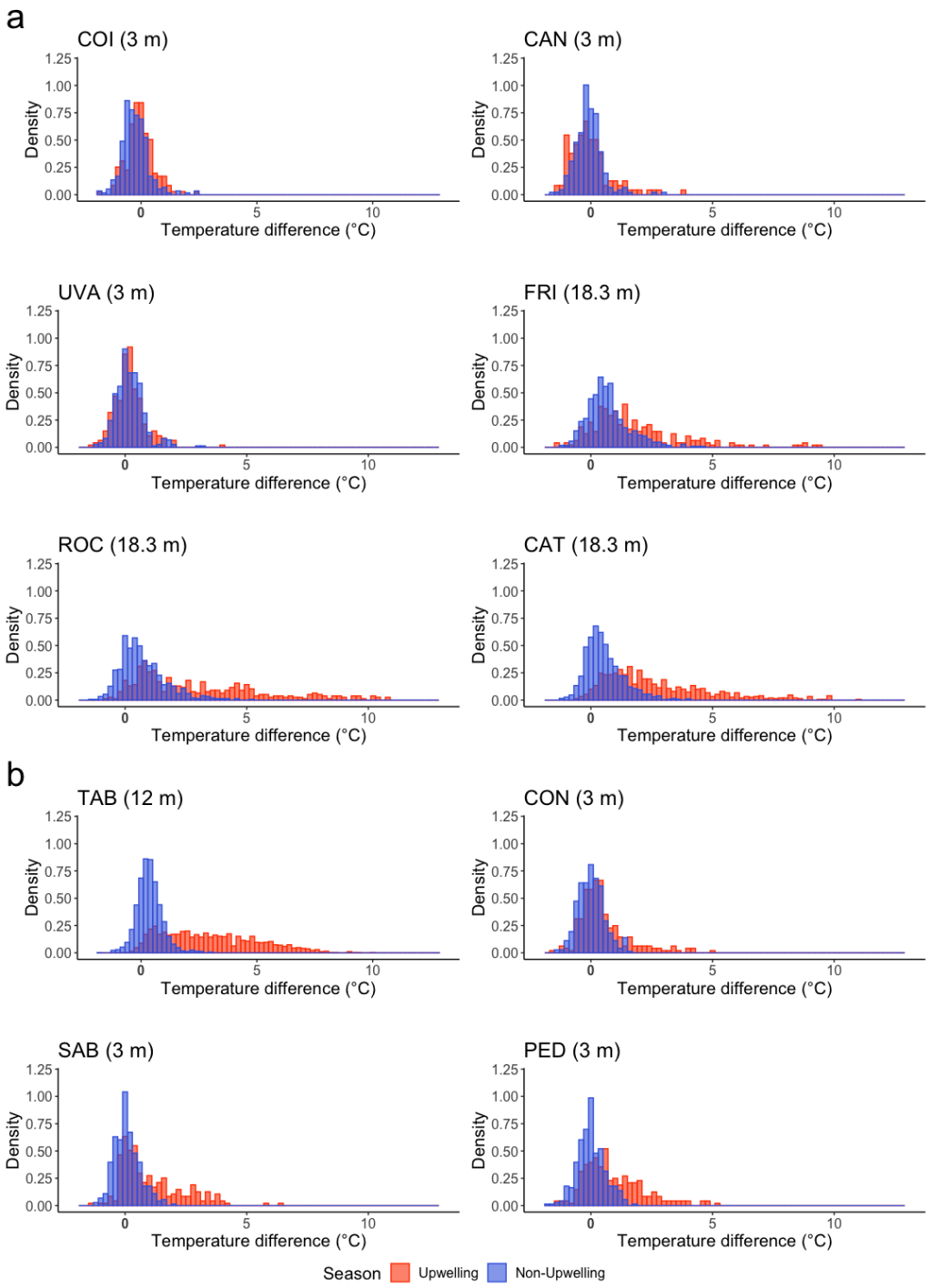

Figure 4. Density plot of daily temperature differences ([fSST - IST]), separated by season for sites in the Pacific. a) Gulf of Chiriquí and b) Gulf of Panama. GAL: Galeta, GRA: Isla Grande, BAH: Bahía Las Minas, BDT: Bocas del Toro Platform, SEA: Isla Colón Seagrass, IC5: Isla Colón 4.6 m, IC9: Isla Colón 9.1 m, IC18: Isla Colón 18.3 m, ICA: Cayo Agua, COI: Coiba, CAN: Canales de Tierra, UVA: Uva, FRI: Isla Coiba Frijoles, ROC: Isla Coiba Roca Hacha, CAT: Isla Jicarón Catedral, TAB: Isla Taboguilla, CON: Contadora, SAB: Saboga, PED: Pedro González.

Table 3. Summary of the linear relationships between logger and MUR satellite data. Results are shown for the entire dataset and subsets of the data for the upwelling (UP; January 1-April 30) and non-upwelling (NU; June 1-November 30) seasons.

Location	Depth (-m)	Pearson's correlation (R)			Linear regression slope		
		Overall	UP	NU	Overall	UP	NU
Caribbean Sea							
Galeta							
Galeta Channel	3	0.79	0.67	0.49	0.80	0.61	0.50
Isla Grande	3	0.88	0.78	0.71	0.92	0.71	0.81
Bahía Las Minas	3	0.84	0.75	0.60	0.88	0.66	0.65
Bocas del Toro							
Bocas del Toro Platform	1	0.85	0.82	0.70	0.76	0.73	0.67
Isla Colón Seagrass	2	0.85	0.85	0.85	0.79	0.79	0.79
Isla Colón	4.6	0.85	0.83	0.70	0.78	0.78	0.70
Isla Colón	9.1	0.83	0.80	0.66	0.76	0.73	0.68
Isla Colón	18.3	0.72	0.69	0.44	0.69	0.81	0.58
Cayo Agua	5.2	0.82	0.77	0.66	0.79	0.91	0.67
Pacific Ocean							
Gulf of Chiriquí							
Coiba	3	0.54	0.70	0.50	0.58	0.54	0.71
Canales de Tierra	3	0.49	0.77	0.22	0.41	0.47	0.41
Uva	3	0.62	0.66	0.58	0.60	0.43	0.71
Isla Coiba Frijoles	18.3	0.42	0.29	0.65	0.27	0.12	0.45
Isla Coiba Roca Hacha	18.3	0.25	0.29	0.67	0.12	0.07	0.45
Isla Jicarón Catedral	18.3	0.27	0.32	0.71	0.14	0.09	0.54
Gulf of Panama							
Isla Taboguilla	12	0.92	0.84	0.55	0.51	0.44	0.62
Contadora	3	0.94	0.91	0.64	0.79	0.69	0.86
Saboga	3	0.93	0.89	0.64	0.72	0.63	0.97
Pedro González	3	0.94	0.90	0.59	0.75	0.67	0.87

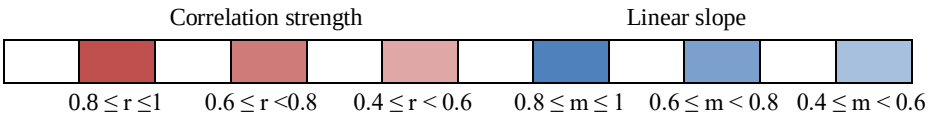

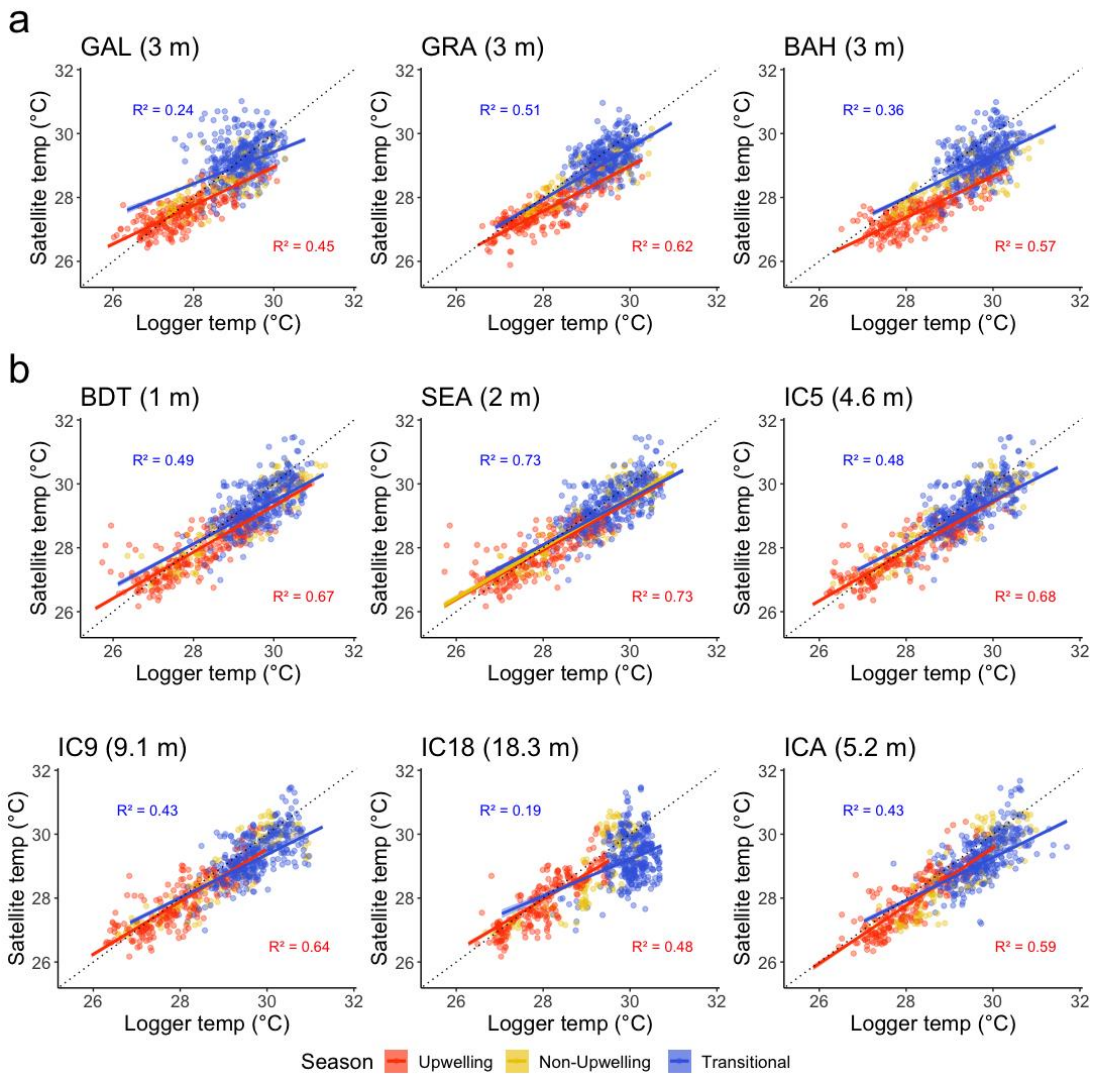

Figure 5. Linear relationships between Caribbean logger and MUR satellite data for sites in a) Galeta and b) Bocas del Toro. Shading indicates the 95% confidence interval of linear model satellite estimates. For all sites, regression lines and r-squared values represent data from the full 2009-2020 dataset, but only points from March 2, 2016 to March 9, 2018 are plotted to avoid overcrowding plots. GAL: Galeta, GRA: Isla Grande, BAH: Bahía Las Minas, BDT: Bocas del Toro Platform, SEA: Isla Colón Seagrass, IC5: Isla Colón 4.6 m, IC9: Isla Colón 9.1 m, IC18: Isla Colón 18.3 m, ICA: Cayo Agua, COI: Coiba, CAN: Canales de Tierra, UVA: Uva, FRI: Isla Coiba Frijoles, ROC: Isla Coiba Roca Hacha, CAT: Isla Jicarón Catedral, TAB: Isla Taboguilla, CON: Contadora, SAB: Saboga, PED: Pedro González.

coastal sites (Leichter et al. 2006, Pearce et al. 2007, Smale & Wernberg 2009, Castillo & Lima 2010, Dufois et al. 2012, Smit et al. 2013, Stobart et al. 2015, Claar et al. 2019, Colin & Johnston 2020, Pereira et al. 2020) and emphasize that this unreliability is of particular concern in upwelling zones. In laboratory studies, organismal performance has been shown to change drastically when exposure temperatures increase by 0.5-1.0°C for only 2 h (Collin et al. 2021). IST monitoring remains the only method to reliably provide habitat temperature estimates with known accuracy and precision, and the only way to capture fine temporal variation (Leichter et al. 2006, 2012, DeCarlo et al. 2015, Lee et al. 2020, Wyatt et al. 2020). Before using satellite data as proxies, researchers should conduct ground-truthing to determine whether there are temperature-dependent or seasonal biases in local conditions and if the accuracy of the satellite data is sufficient for their purposes. However, when this is impossible, our data suggest that MUR can provide

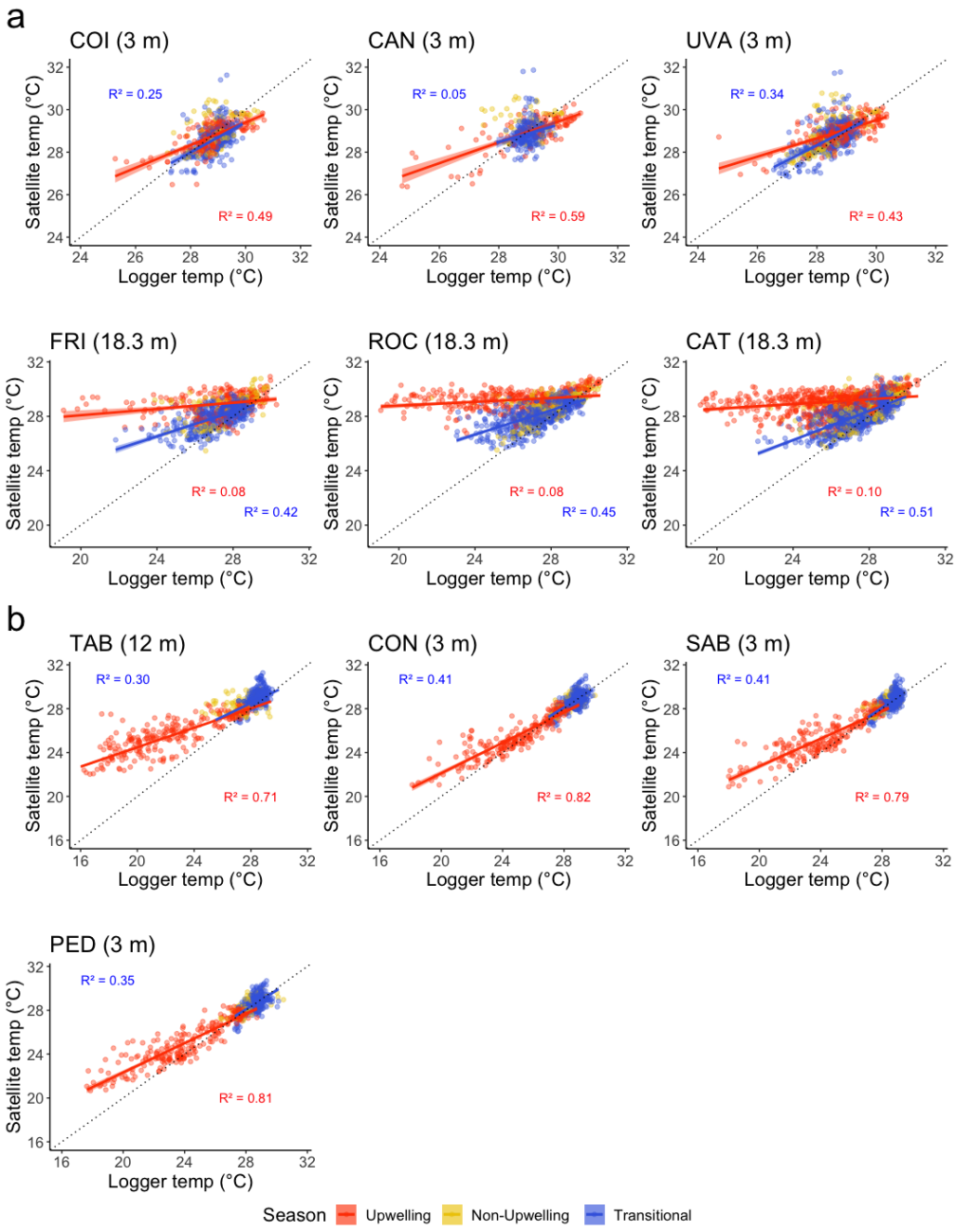

Figure 6. Linear relationships between Pacific logger and MUR satellite data for sites in a) the Gulf of Chiriquí and b) the Gulf of Panama. Shading indicates a 95% confidence interval of linear model satellite estimates. For TAB, regression lines and r-squared values represent data from the full 2009-2020 dataset, but only points from March 2, 2016 to March 9, 2018 are plotted to avoid overcrowding plots. Temperatures below 24, 19, and 16°C are not plotted for a), b), and c), respectively. GAL: Galeta, GRA: Isla Grande, BAH: Bahía Las Minas, BDT: Bocas del Toro Platform, SEA: Isla Colón Seagrass, IC5: Isla Colón 4.6 m, IC9: Isla Colón 9.1 m, IC18: Isla Colón 18.3 m, ICA: Cayo Agua, COI: Coiba, CAN: Canales de Tierra, UVA: Uva, FRI: Isla Coiba Frijoles, ROC: Isla Coiba Roca Hacha, CAT: Isla Jicarón Catedral, TAB: Isla Taboguilla, CON: Contadora, SAB: Saboga, PED: Pedro González.

fairly reliable temperature estimates in shallow tropical waters that are not experiencing upwelling.

ACKNOWLEDGEMENTS

We thank Steve Paton and the STRI Environmental Monitoring Program for sharing their temperature data and the Government of the Republic of Panama for granting permission to collect environmental data. We further thank Carly Randall, Lauren Toth, James Leichter, Juan Maté, and Richard Aronson for sharing the coordinates of their published logger data with us. A STRI internship supported FS. On behalf of all authors, the corresponding author states that there is no conflict of interest. The Smithsonian Tropical Research Institute supported this work.

REFERENCES

Adelson, A.E., Altieri, A.H., Boza, X., Collin, R., Davis, K.A., Gaul, A., et al. 2022. Seasonal hypoxia and temperature inversions in a tropical bay. Limnology and Oceanography, 67: 2174-2189. doi: 10.1002/lno.12196

Alderdice, R., Perna, G., Cárdenas, A., Hume, B.C., Wolf, M., Kühl, M., et al. 2022. Deoxygenation lowers the thermal threshold of coral bleaching. Scientific Reports, 12: 18273. doi: 10.1038/s41598-022-22604-3

Andréfouët, S. & Guzmán, H.M. 2005. Coral reef distribution, status and geomorphology-biodiversity relationship in Kuna Yala (San Blas) archipelago, Caribbean Panama. Coral Reefs, 24: 31-42. doi: 10.1007/s00338-004-0444-4

Bahr, K.D., Tran, T., Jury, C.P. & Toonen, R.J. 2020. Abundance, size, and survival of recruits of the reef coral *Pocillopora acuta* under ocean warming and acidification. Plos One, 15: e0228168. doi: 10.1371/journal.pone.0228168

Bailey, K., Steinberg, C., Davies, C., Galibert, G., Hidas, M., McManus, M., et al. 2019. Coastal mooring observing networks and their data products: Recommendations for the next decade. Frontiers in Marine Science, 6: 180. doi: 10.3389/fmars.2019.00180

Bennett, S., Alcoverro, T., Kletou, D., Charalampos, A., Boada, J., Buñuel, X., et al. 2022. Resilience of seagrass populations to thermal stress does not reflect regional differences in ocean climate. New Phytologist, 233: 1657-1666. doi: 10.1111/nph.17885

Benway, H.M., Lorenzoni, L., White, A.E., Fiedler, B., Levine, N., Nicholson, D., et al. 2019. Ocean time series observations of changing marine ecosystems: An era of integration, synthesis, and societal applications. Frontiers in Marine Science, 6: 393. doi: 10.3389/fmars.2019 .00393

Castillo, K.D. & Lima, F.P. 2010. Comparison of in situ and satellite-derived (MODIS-Aqua/Terra) methods for assessing temperatures on coral reefs. Limnology and Oceanography: Methods, 8: 107-117. doi: 10.4319/lom.2010.8.0107

Chin, T.M., Vazquez-Cuervo, J. & Armstrong, E.M. 2017. A multiscale high-resolution analysis of global sea surface temperature. Remote Sensing of Environment, 200: 154-169. doi: 10.1016/j.rse.2017.07.029

Claar, D.C., Cobb, K.M. & Baum, J.K. 2019. *In situ* and remotely sensed temperature comparisons on a Central Pacific atoll. Coral Reefs, 38: 1343-1349. doi: 10.1007/s00338-019-01850-4

Colin, P.L. & Johnston, T.S. 2020. Measuring temperature in coral reef environments: experience, lessons, and results from Palau. Journal of Marine Science and Engineering, 8: 680. doi: 10.3390/jmse8090680

Collin, R. & Chan, K.Y.K. 2016. The sea urchin *Lytechinus variegatus* lives close to the upper thermal limit for early development in a tropical lagoon. Ecology and Evolution, 6: 5623-5634. doi: 10.1002/ece3.2317

Collin, R., Rebolledo, A.P., Smith, E. & Chan, K.Y.K. 2021. Thermal tolerance of early development predicts the realized thermal niche in marine ectotherms. Functional Ecology, 35: 1679-1692. doi: 10.1111/1365-2435.13850

Contractor, S. & Roughan, M. 2021. Efficacy of reedforward and LSTM neural networks at predicting and gap-filling coastal ocean time series: Oxygen, nutrients, and temperature. Frontiers in Marine Science, 8: 637759. doi: 10.3389/fmars.2021.637759

Cornwall, C.E., Comeau, S., Kornder, N.A., Perry, C.T., Hooidonk, R.V., DeCarlo, T.M., et al. 2021. Global declines in coral reef calcium carbonate production under ocean acidification and warming. Proceedings of the National Academy of Sciences, 118: e2015265118. doi: 10.1073/pnas.2015265118

Cyronak, T., Takeshita, Y., Courtney, T.A., DeCarlo, E.H., Eyre, B.D., Kline, D.I., et al. 2020. Diel temperature and pH variability scale with depth across diverse coral reef habitats. Limnology and Oceanography Letters, 5: 193-203. doi: 10.1002/lol2.10129

Dash, P., Ignatov, A., Martin, M., Donjon, C., Brasnett, B., Reynolds, R., et al. 2012. Group for High Resolution Sea Surface Temperature (GHRSST) analysis fields inter-comparisons-Part 2: Near real-time web-based level 4 SST Quality Monitor (L4-SQUAM). Deep Sea Research - Part II: Topical Studies in Oceanography, 77: 31-43. doi: 10.1016/j.dsr2.2012.04.002

D'Croz, L. & O'Dea, A. 2007. Variability in upwelling along the Pacific shelf of Panama and implications for the distribution of nutrients and chlorophyll. Estuarine, Coastal and Shelf Science, 73: 325-340. doi: 10.1016/j.ecss.2007.01.013

DeCarlo, T.M., Karnauskas, K.B., Davis, K.A. & Wong, G.T. 2015. Climate modulates internal wave activity in the northern south China Sea. Geophysical Research Letters, 42: 831-838. doi: 10.1002/2014GL062522

Dominici-Arosemena, A. & Wolff, M. 2005. Reef fish community structure in Bocas del Toro (Caribbean, Panama): gradients in habitat complexity and exposure. Caribbean Journal of Science, 41: 613-637.

Dufois, F., Penven, P., Whittle, C.P. & Veitch, J. 2012. On the warm nearshore bias in Pathfinder monthly SST products over Eastern Boundary Upwelling Systems. Ocean Modelling, 47: 113-118. doi: 10.1016/j.ocemod.2012.01.007

Enochs, I.C., Toth, L.T., Kirkland, A., Manzello, D.P., Kolodziej, G., Morris, J.T., et al. 2021. Upwelling and the persistence of coral-reef frameworks in the eastern tropical Pacific. Ecological Monographs, 91: 01482. doi: 10.1002/ecm.1482

Furnas, M.J. 2011. Upwelling and coral reefs. In: Hopley, D. (Ed.). Encyclopedia of modern coral reefs. Springer, Berlin, pp. 1125-1132.

Gardner, T.A., Côté, I.M., Gill, J.A., Grant, A. & Watkinson, A.R. 2003. Long-term region-wide declines in Caribbean corals. Science, 301: 958-960. doi: 10.1126/science.1086050

Gomez, C.G., Gonzalez, A. & Guzmán, H.M. 2017. Multiscale change in reef coral species diversity and composition in the Tropical Eastern Pacific. Coral Reefs, 37: 105-120. doi: 10.1007/s00338-017-1637-y

Gomez, A.M., McDonald, K.C., Shein, K., DeVries, S., Armstrong, R.A., Hernandez, W.J., et al. 2020. Comparison of satellite-based sea surface temperature to *in situ* observations surrounding coral reefs in La Parguera, Puerto Rico. Journal of Marine Science and Engineering, 8: 453. doi: 10.3390/jmse8060453

Grantham, B.A., Chan, F., Nielsen, K.J., Fox, D.S., Barth, J.A., Huyer, A., et al. 2004. Upwelling-driven nearshore hypoxia signals ecosystem and oceanographic changes in the northeast Pacific. Nature, 429: 749-754. doi: 10.1038/nature02605

Guzmán, H.M. 2003. Caribbean coral reefs of Panama: present status and future perspectives. Latin American Coral Reefs, 2003: 241-274. doi: 10.1016/B978-0444513885/50012-6

Guzmán, H.M., Kaiser, S. & Weil, E. 2020. Assessing the long-term effects of a catastrophic oil spill on subtidal coral reef communities off the Caribbean coast of Panama (1985-2017). Marine Biodiversity, 50: 1-19. doi: 10.1007/s12526-020-01057-9

Hedley, J.D., Roelfsema, C.M., Chollett, I., Harborne, A.R., Heron, S.F., Weeks, S., et al. 2016. Remote sensing of coral reefs for monitoring and management: A review. Remote Sensing, 8: 118. doi: 10.3390/rs8020118

Hemming, M.P., Roughan, M. & Schaeffer, A. 2020. Daily subsurface ocean temperature climatology using multiple data sources: New methodology. Frontiers in Marine Science, 7: 485. doi: 10.3389/fmars.2020.00485

Hughes, T.P., Kerry, J.T., Baird, A.H., Connolly, S.R., Dietzel, A., Eakin, C.M., et al. 2018. Global warming transforms coral reef assemblages. Nature, 556: 492-496. doi: 10.1038/s41586-018-0041-2

JPL MUR MEASUREs Project. 2015. GHRSST Level 4 MUR Global Foundation Sea Surface Temperature Analysis (v4.1). PO.DAAC. [https://podaac.jpl.nasa.gov/dataset/MUR-JPL-L4-GLOB-v4.1]. Reviewed: February 4, 2023.

Kaufmann, K. & Thompson, R.C. 2005. Water temperature variation and the meteorological and hydrographic environment of Bocas del Toro, Panama. Caribbean Journal of Science, 41: 392-413.

Klepac, C.N. & Barshis, D.J. 2022. High-resolution *in situ* thermal metrics coupled with acute heat stress experiments reveal differential coral bleaching susceptibility. Coral Reefs, 41: 1045-1057. doi: 10.1007/s00338-022-02276-1

Largier, J.L. 2020. Upwelling bays: How coastal upwelling controls circulation, habitat, and productivity in bays. Annual Review of Marine Science, 12: 415-447. doi: 10.1146/annurev-marine-010419-011020

Lee, I.H., Fan, T.Y., Fu, K.H. & Ko, D.S. 2020. Temporal variation in daily temperature minima in coral reefs of Nanwan Bay, Southern Taiwan. Scientific Reports, 10: 8656. doi: 10.1038/s41598-020-65194-8

Leichter, J.J., Helmuth, B. & Fischer, A.M. 2006. Variation beneath the surface: Quantifying complex

thermal environments on coral reefs in the Caribbean, Bahamas, and Florida. Journal of Marine Research, 64: 563-588. doi: 10.1357/002224006778715711

Leichter, J.J., Stokes, M.D., Hench, J.L., Witting, J. & Washburn, L. 2012. The island-scale internal wave climate of Moorea, French Polynesia. Journal of Geophysical Research: Oceans, 117: 1-16. doi: 10.1029/2012JC007949

Liu, G., Heron, S.F., Eakin, C.M., Muller-Karger, F.E., Vega-Rodriguez, M., Guild, L.S., et al. 2014. Reef-scale thermal stress monitoring of coral ecosystems: New 5-km global products from NOAA Coral Reef Watch. Remote Sensing, 6: 11579-11606. doi: 10.3390/rs61111579

Lough, J.M., Anderson, K.D. & Hughes, T.P. 2018. Increasing thermal stress for tropical coral reefs: 1871-2017. Scientific Reports, 8: 1-8. doi: 10.1038/s41598-018-24530-9

Lucey, N.M., Haskett, E. & Collin, R. 2021. Hypoxia from depth shocks shallow tropical reef animals. Climate Change Ecology, 2: 100010. doi: 10.1016/j.ecochg.2021.100010

Manzello, D.P., Kleypas, J.A., Budd, D.A., Eakin, C.M., Glynn, P.W. & Langdon, C. 2008. Poorly cemented coral reefs of the eastern tropical Pacific: Possible insights into reef development in a high-CO2 world. Proceedings of the National Academy of Sciences, 105: 10450-10455. doi: 10.1073/pnas.0712167105

Marbà, N., Jordà, G., Bennett, S. & Duarte, C.M. 2022. Seagrass thermal limits and vulnerability to future warming. Frontiers in Marine Science, 9: 860826. doi: 10.3389/fmars.2022.860826

Neal, B.P., Khen, A., Treibitz, T., Beijbom, O., O'Connor, G., Coffroth, M.A., et al. 2017. Caribbean massive corals not recovering from repeated thermal stress events during 2005-2013. Ecology and Evolution, 7: 339-1353. doi: 10.1002/ece3.2706

O'Dea, A., Hoyos, N., Rodríguez, F., Degracia, B. & De Gracia, C. 2012. History of upwelling in the Tropical Eastern Pacific and the paleogeography of the Isthmus of Panama. Paleogeography, Paleoclimatology, Palaeoecology, 348: 59-66. doi: 10.1016/j.palaeo.2012.06.007

Pearce, A., Faskel, F. & Hyndes, G. 2007. Nearshore sea temperature variability off Rottnest Island (Western Australia) derived from satellite data. International Journal of Remote Sensing, 27: 2503-2518. doi: 10.1080/01431160500472138

Pereira, F., Bouali, M., Polito, P.S., Da Silveira, I.C.A. & Candella, R.N. 2020. Discrepancies between satellite-derived and *in situ* SST data in the Cape Frio Upwelling System, Southeastern Brazil (23°S). Remote Sensing Letters, 11: 555-562. doi: 10.1080/2150704X.2020.1742941

Peres, L.F., França, G.B., Paes, R.C., Sousa, R.C. & Oliveira, A.N. 2017. Analyses of the positive bias of remotely sensed SST retrievals in the coastal waters of Rio de Janeiro. IEEE Transactions on Geoscience and Remote Sensing, 55: 6344-6353. doi: 10.1109/TGRS.2017.2726344

Randall, C.J., Toth, L.T., Leichter, J.J., Maté, J.L. & Aronson, R.B. 2020. Upwelling buffers climate change impacts on coral reefs of the eastern tropical Pacific. Ecology, 101: e02918. doi: 10.1002/ecy.2918

Robertson, D.R. & Collin, R. 2015. Inter-and intra-specific variation in egg size among reef fishes across the Isthmus of Panama. Frontiers in Ecology and Evolution, 2: 84. doi: 10.3389/fevo.2014.0008

Rodas, A.M., Wright, R.M., Buie, L.K., Aichelman, H.E., Castillo, K.D. & Davies, S.W. 2020. Eukaryotic plankton communities across reef environments in Bocas del Toro Archipelago, Panamá. Coral Reefs, 39: 1453-1467. doi: 10.1007/s00338-020-01979-7

Savva, I., Bennett, S., Roca, G., Jordà, G. & Marbà, N. 2018. Thermal tolerance of Mediterranean marine macrophytes: Vulnerability to global warming. Ecology and Evolution, 8: 12032-12043. doi: 10.1002/ece3.4663

Seemann, J., González, C.T., Carballo-Bolaños, R., Berry, K., Heiss, G.A., Struck, U. & Leinfelder, R.R. 2013. Assessing the ecological effects of human impacts on coral reefs in Bocas del Toro, Panama. Environmental Monitoring and Assessment, 186: 1747-1763. doi: 10.1007/s10661-013-3490-y

Sellers, A.J., Leung, B., Altieri, A.H., Glanz, J., Turner, B.L. & Torchin, M.E. 2021. Seasonal upwelling reduces herbivore control of tropical rocky intertidal algal communities. Ecology, 102: e03335. doi: 10.1002/ecy.3335

Shulman, M.J. & Robertson, D.R. 1996. Changes in the coral reefs of San Blas, Caribbean Panama: 1983 to 1990. Coral Reefs, 15: 231-236. doi: 10.1007/BF01787457

Smale, D.A. & Wernberg, T. 2009. Satellite-derived SST data as a proxy for water temperature in nearshore benthic ecology. Marine Ecology Progress Series, 387: 27-37. doi: 10.3354/meps 08132

Smit, A.J., Roberts, M., Anderson, R.J., Dufois, F., Dudley, S.F., Bornman, T.G., et al. 2013. A coastal seawater temperature dataset for biogeographical

studies: Large biases between *in situ* and remotely-sensed data sets around the coast of South Africa. Plos One, 8: e81944. doi: 10.1371/journal.pone.0081944

Stobart, B., Mayfield, S., Mundy, C., Hobday, A.J. & Hartog, J.R. 2015. Comparison of *in situ* and satellite sea surface-temperature data from South Australia and Tasmania: How reliable are satellite data as a proxy for coastal temperatures in temperate southern Australia? Marine and Freshwater Research, 67: 612-625. doi: 10.1071/MF14340

Toth, L.T., Macintyre, I.G. & Aronson, R.B. 2017. Holocene reef development in the Eastern Tropical Pacific. In: Glynn, P., Manzello, D. & Enochs, I. (Eds.). Coral reefs of the Eastern Tropical Pacific. Springer, Berlin, pp. 177-201.

Vazquez-Cuervo, J., Gomez-Valdes, J., Bouali, M., Miranda, L.E., Van der Stocken, T., Tang, W., et al. 2019. Using saildrones to validate satellite-derived sea surface salinity and sea surface temperature along the California/Baja coast. Remote Sensing, 11: 1964. doi: 10.3390/rs11171964

Received: June 20, 2023; Accepted: November 27, 2023

Vinagre, C., Mendonca, V., Cereja, R., Abreu-Afonso, F., Dias, M., Mizrahi, D., et al. 2018. Ecological traps in shallow coastal waters - Potential effect of heat waves in tropical and temperate organisms. Plos One, 13: e0192700. doi: 10.1371/journal.pone.0192700

Woo, H.J. & Park, K. 2020. Inter-comparisons of daily sea surface temperatures and *in-situ* temperatures in the coastal regions. Remote Sensing, 12: 1592. doi: 10.3390/rs12101592

Wyatt, A.S., Leichter, J.J., Toth, L.T., Miyajima, T., Aronson, R.B. & Nagata, T. 2020. Heat accumulation on coral reefs mitigated by internal waves. Nature Geoscience, 13: 28-34. doi: 10.1038/s41561-019-0486-4

Table S1. Summary statistics of daily temperature differences between loggers and MUR satellite data with additional breakdown by upwelling (UP; January 1-April 30) and non-upwelling (NU; June 1-November 30) season. Negative temperature values indicate an underestimate of *in situ* temperature by MUR satellite temperature, and positive temperature values indicate an overestimate.

Location	Depth (-m)	Skew			Kurtosis		Median (ºC)			Min (ºC)			Max (ºC)	
		Overall	UP	NU	Overall	UP	NU	Overall	UP	NU	UP	NU	UP	NU
Caribbean Sea														
Galeta														
Galeta Channel	3	0.33	0.03	0.52	4.19	4.13	4.02	-0.09	-0.10	-0.10	-2.39	-1.92	2.22	2.35
Isla Grande	3	-0.07	-0.56	0.19	3.70	3.18	3.65	-0.31	-0.34	-0.29	-1.83	-2.04	0.59	1.98
Bahía Las Minas	3	0.04	-0.17	0.11	3.55	3.11	3.50	-0.55	-0.65	-0.51	-2.19	-2.27	0.82	1.67
Bocas del Toro														
Bocas del Toro Platform	1	0.20	0.61	0.11	3.94	5.40	3.34	-0.23	-0.17	-0.30	-1.76	-2.13	2.75	2.06
Isla Colon Seagrass	2	0.10	0.61	0.01	3.69	5.20	2.95	-0.19	-0.11	-0.25	-1.58	-1.95	2.85	1.55
Isla Colon	4.6	-0.09	0.62	-0.26	4.33	5.19	3.78	-0.20	-0.14	-0.27	-1.62	-2.71	2.12	1.62
Isla Colon	9.1	-0.20	0.63	-0.25	3.81	4.36	3.33	-0.29	-0.17	-0.44	-1.29	-2.70	2.08	1.61
Isla Colon	18.3	-0.09	0.73	-0.08	3.31	4.10	2.89	-0.37	-0.08	-0.61	-1.33	-3.31	2.20	1.40
Cayo Agua	5.2	0.04	0.7	-0.11	4.13	4.37	4.07	-0.45	-0.30	-0.58	-1.61	-3.35	1.89	1.37
Pacific Ocean														
Gulf of Chiriquí														
Coiba	3	0.84	0.53	1.03	4.73	4.60	6.52	-0.18	-0.06	-0.32	-1.74	-1.85	2.43	2.31
Canales de Tierra	3	1.44	1.52	1.36	6.49	6.22	8.86	-0.10	-0.16	-0.11	-1.48	-1.53	3.70	2.98
Uva	3	1.16	1.26	1.07	6.54	8.04	6.25	0.16	0.14	0.14	-1.41	-1.16	4.01	3.13
Isla Coiba Frijoles	18.3	2.22	1.56	1.10	10.94	6.04	5.11	0.70	1.36	0.55	-1.44	-1.26	9.35	4.68
Isla Coiba Roca Hacha	18.3	2.16	0.95	1.18	8.24	3.11	5.09	0.80	2.32	0.53	-0.71	-1.48	10.77	5.21
Isla Jicarón Catedral	18.3	2.13	1.16	1.05	8.58	4.00	4.67	0.73	2.07	0.40	-0.51	-1.29	11.01	4.08
Bay of Panama														
Isla Taboguilla	12	1.74	0.51	0.58	5.69	2.50	5.66	0.59	2.68	0.32	-0.84	-2.66	10.03	3.06
Contadora	3	2.00	1.60	0.35	10.30	6.13	3.24	0.09	0.25	0.02	-1.66	-1.34	5.06	1.59
Saboga	3	1.99	1.12	0.54	8.57	4.08	3.49	0.16	0.56	0.04	-1.35	-1.20	6.42	2.04
Pedro Gonzalez	3	1.65	0.97	0.15	7.44	3.88	3.26	0.13	0.58	-0.02	-1.46	-1.72	5.18	1.71

Table S2. Daily temperature differences (DTDs) averaged by month for each site. Negative values indicate an underestimate of *in situ* temperature by MUR satellite temperature, and positive temperature values indicate an overestimate. Values of NA indicate months of missing data.

Location	Mean DTD (ºC)											
	Jan	Feb	March	April	May	June	July	Aug	Sept	Oct	Nov	Dec
Galeta Channel	0.23	-0.08	-0.28	-0.39	-0.10	-0.17	-0.11	-0.10	0.03	0.01	0.00	-0.02
Isla Grande	-0.15	-0.31	-0.52	-0.56	-0.32	-0.28	-0.30	-0.24	-0.29	-0.28	-0.36	-0.27
Bahía Las Minas	-0.33	-0.67	-0.82	-0.89	-0.52	-0.56	-0.50	-0.43	-0.38	-0.53	-0.56	-0.45
Bocas del Toro Platform	-0.05	-0.16	-0.16	-0.30	-0.34	-0.49	-0.27	-0.20	-0.25	-0.37	-0.29	-0.03
Isla Colon Seagrass	0.00	-0.07	-0.08	-0.18	-0.28	-0.48	-0.26	-0.14	-0.15	-0.28	-0.28	-0.03
Isla Colon (4.6m)	-0.03	-0.10	-0.12	-0.23	-0.28	-0.47	-0.30	-0.17	-0.28	-0.37	-0.23	0.01
Isla Colon (9.1 m)	-0.13	-0.12	-0.09	-0.16	-0.23	-0.57	-0.55	-0.30	-0.39	-0.54	-0.46	-0.16
Isla Colon (18.3 m)	-0.20	-0.06	-0.03	0.08	0.00	-0.48	1.02	-0.42	-0.19	-0.54	-1.07	-0.61
Cayo Agua	-0.43	-0.29	-0.17	-0.12	-0.23	-0.57	-0.60	-0.55	-0.54	-0.67	-0.59	-0.48
Coiba	-0.09	-0.05	-0.03	-0.01	0.34	-0.05	-0.25	-0.52	-0.20	-0.14	-0.39	-0.34
Canales de Tierra	NA	NA	0.03	-0.10	0.36	0.06	-0.10	-0.34	0.08	NA	NA	NA
Uva	0.12	0.07	0.40	0.13	0.64	0.32	0.17	-0.12	0.33	0.44	0.05	0.22
Isla Coiba Frijoles	0.98	2.08	2.31	1.83	1.34	0.47	0.49	0.74	0.86	0.89	0.69	0.66
Isla Coiba Roca Hacha	1.41	3.59	4.09	3.69	1.29	0.87	0.68	0.70	0.76	0.86	0.47	0.55
Isla Jicarón Catedral	1.38	2.81	3.52	3.21	1.19	0.42	0.35	0.50	0.72	0.76	0.52	0.49
Isla Taboguilla	1.67	3.58	3.86	2.52	0.78	0.32	0.36	0.48	0.45	0.25	0.28	0.52
Contadora	0.10	0.88	0.57	0.54	0.07	-0.10	-0.17	-0.01	0.29	0.14	-0.05	0.08
Saboga	0.23	1.52	1.31	1.22	0.34	-0.06	-0.01	0.14	0.39	0.09	-0.09	0.09
Pedro Gonzalez	0.18	1.45	1.29	0.81	0.24	-0.09	0.01	0.15	0.26	-0.02	-0.27	0.06